

# Multiparameter collaborative optimization of the vibrating screen based on the behavior of oil sunflower seed penetrating screen holes

Wenbo Wei<sup>1,2†</sup>, Jianchang Li<sup>1†</sup>, Jianjun Hao<sup>1\*</sup>, Maohua Xiao<sup>2</sup>, Huiju Zhang<sup>3</sup>

(1. College of Mechanical and Electrical Engineering, Hebei Agricultural University, Baoding 071001, Hebei, China;

2. College of Engineering, Nanjing Agricultural University, Nanjing 210032, China;

3. The Higher Educational Key Laboratory for Flexible Manufacturing Equipment Integration of Fujian Province, Xiamen Institute of Technology, Xiamen 361000, Fujian, China)

**Abstract:** The behavior of oil sunflower seeds penetrating screen holes is an important factor that affects the screening performance of oil sunflower seeds. In this study, a double-deck reverse-motion vibrating screening device for oil sunflower seed screening was designed. The force condition and motion law of the oil sunflower seeds on the screen surface were analyzed. This study compared the effect of particle filling amount of discrete element model of oil sunflower seeds on the simulation effects. The screening process was numerically simulated using the coupled Discrete Element Method and Multibody Dynamics (DEM-MBD) technique with the screening percentage of oil sunflower seeds as the index. The influence of the operating parameters of the vibrating screen on the screening effect was analyzed using a multiparameter collaborative optimization scheme. The results of this study can provide a reference for the numerical simulation of crop screening behavior and the development of screening devices.

**Keywords:** oil sunflower seeds, screening analysis, DEM-MBD, discrete element method, response surface analysis

**DOI:** [10.25165/j.ijabe.20241701.8111](https://doi.org/10.25165/j.ijabe.20241701.8111)

**Citation:** Wei W B, Li J C, Hao J J, Xiao M H, Zhang H J. Multiparameter collaborative optimization of the vibrating screen based on the behavior of oil sunflower seed penetrating screen holes. *Int J Agric & Biol Eng*, 2024; 17(1): 49–58.

## 1 Introduction

Sunflower is a tall annual herbaceous plant that is very tolerant to drought and alkali and has good adaptability to soil, making it one of the world's major oil crops<sup>[1,2]</sup>. The screening process of oil sunflower seeds is an important factor to ensure the harvest quality of oil sunflower seeds. As a key component of the oil sunflower seed screening device, the structure and working parameters of the vibrating screen have an important impact on the screening performance. Through the numerical simulation of the crop screening process, statistical analysis of, for example, crop movement speed, movement direction, collision, and force determines the interaction between the crop and the screening equipment to provide a reference for the optimization of the screening equipment. Numerical simulation analysis of the behavior of oil sunflower seeds through the screen is beneficial to fully understand the movement process of oil sunflower seeds on the vibrating screen and has the advantages of low cost and high efficiency. Therefore, it is important to optimize the vibrating screen structure and working parameters in a targeted way to

improve the screening percentage and decrease the screening loss.

In recent years, Discrete Element Method (DEM) has been widely used for research in the field of vibratory screening. Currently, many scholars use the DEM to study the influence of the working parameters of the vibrating screen on the screening performance and to clarify the relationship between the working parameters and the screening performance to optimize the screening effect. For example, Chen et al.<sup>[3]</sup> numerically simulated the screening process of an elliptically vibrating screen based on EDEM software, and their results indicate that the vibration frequency and the inclination angle had a significant effect on the screening efficiency and screening time. Yin et al.<sup>[4]</sup> used EDEM software to numerically simulate the elliptically vibrating screen and quantitatively analyze the variation law of screening efficiency with vibration parameters, and their results indicate that the screening efficiency was mainly influenced by the delamination rate and contact opportunity (the collision time between particles and the screen surface). Liu et al.<sup>[5]</sup> used EDEM software to numerically simulate the particle flow on a banana screen and approximated the relationship between screen surface length and screening efficiency using the Boltzmann equation. Yang et al.<sup>[6]</sup> simulated the screening process of an industrial-scale roller screen based on the DEM. In addition, they analyzed the variation law of screening efficiency with working parameters and the influence of particle shape and cohesion force between wet particles on the screening process. Moreover, some scholars use the DEM to analyze the screening process and particle motion state of different types of vibrating screens and propose relevant screening theories. For example, Wang et al.<sup>[7]</sup> analyzed the motion state of maize particle clusters on the screen surface in different motion forms based on particle nonlinear hopping theory and explored the sieving performance of the screen surface in different motion forms. Xiao et al.<sup>[8]</sup> proposed a new type of screen surface motion based on the principle of manual

Received date: 2022-12-23 Accepted date: 2023-12-06

**Biographies:** Wenbo Wei, PhD candidate, research interest: multi-machine collaboration of agricultural equipment, Email: [wbolear@stu.njau.edu.cn](mailto:wbolear@stu.njau.edu.cn); Jianchang Li, Master, Assistant Research Fellow, research interest: agricultural mechanization engineering, Email: [xuekemishu@163.com](mailto:xuekemishu@163.com); Maohua Xiao, PhD, Professor, research interest: unmanned agricultural equipment, Email: [xiaomaohua@njau.edu.cn](mailto:xiaomaohua@njau.edu.cn); Huiju Zhang, Master, Associate Professor, research interest: stamping and numerical simulation, Email: [307787273@qq.com](mailto:307787273@qq.com).

†These authors contributed equally to this work.

\*Corresponding author: Jianjun Hao, PhD, Professor, research interest: agricultural mechanization engineering. College of Mechanical and Electrical Engineering, Hebei Agricultural University, No. 289, Lingyu Temple Street, Baoding City, Hebei, China. Tel: +86-312-7526451, Fax: +86-312-7521586, Email: [hjj@hebau.edu.cn](mailto:hjj@hebau.edu.cn).

screening, using the irregular motion of the cam to simulate the action of manual screening, and established the equation of motion of the screen surface. Harzanagh et al.<sup>[9]</sup> performed numerical simulations of particles in a vibrating screen by using discrete element models of spherical and nonspherical particles and analyzed the effect of vibrating screen parameters on the screening performance. Ma et al.<sup>[10]</sup> studied the form of motion of the variable amplitude screening mechanism and analyzed the motion of particles on the variable amplitude screening mechanism. Zhao et al.<sup>[11]</sup> investigated the relationship between particle velocity and screening capacity by using spherical and nonspherical particles based on the Taguchi orthogonal experimental design, and they determined the optimal parameters of the vibrating screen. The aforementioned scholars used the DEM to study the screening process of the vibrating screen, the optimization of working parameters, and the motion state of the particle population. The feasibility of optimizing the screening performance of the vibrating screen based on the DEM is fully demonstrated.

In addition, some scholars use the DEM and other simulation methods for coupling analysis to study the influence of vibrating screen operating parameters on each evaluation index. For example, Feng et al.<sup>[12]</sup> developed a kinetic model of particles on a screen based on the center of mass of irregular particles. Discrete Element Method and Computational Fluid Dynamics (DEM-CFD) was used to analyze the motion of maize particles at different stages of screening and the effect of airflow velocity above the sieve on the dispersion degree of particles. Wang et al.<sup>[13]</sup> used the coupled Discrete Element Method and Multibody Kinematics (DEM-MBK) model to simulate the motion of soybeans on a swing-bar screen. Xia et al.<sup>[14]</sup> used the coupled Discrete Element Method and Finite Element Method (DEM-FEM) numerical method to simulate the interaction between the particles and the screen surface, and they analyzed the stress and screen deformation on the screen surface. Wang et al.<sup>[15]</sup> used the coupled DEM-CFD technique to compare the airflow fields of different woven screens and the screening characteristics of different areas. In summary, scholars have demonstrated the feasibility and superiority of the DEM in investigating the effects of structure and operating parameters on the effectiveness of screening equipment. However, many studies have used a case-by-case optimization strategy in optimizing the operating parameters of the vibrating screen, but relatively limited research has been conducted on the collaborative optimization of multiple parameters. In addition, the material is approximated as an ideal sphere in the simulation analysis, and there are relatively few studies on the influence of the model on the simulation effect. Therefore, it is important to investigate the influence of the model on the simulation effect and the multiparameter collaborative optimization of the vibrating screen. The purpose of this study is to clarify the relationship between the behavior of oil sunflower seed penetrating screen holes and the working parameters of vibrating screen, and to carry out the multi-parameter collaborative optimization of the working parameters of vibrating screen based on this relationship. Firstly, based on the inverse modeling technology and EDEM software, a discrete element model of oil sunflower seeds filled by different particle amounts was established to compare the influence of particle filling amount on the simulation effect. Then, a pendulum-type double-deck vibrating screen was designed for the screening of oil sunflower debris, and a simplified simulation model of double-deck vibrating screen was established. Finally, numerical simulation of this vibrating screen was carried out based on DEM and Multibody Dynamics (DEM-MBD)

coupling technology, and the influence of vibrating screen working parameters on the screening percentage of oil sunflower seeds was analyzed through single-factor test and multi-parameter co-optimization test. The results of the study can provide a reference for the research and development of oil sunflower screening equipment and numerical simulation.

## 2 Materials and methods

### 2.1 Discrete element model of oil sunflower seed

A discrete element model of oil sunflower seeds was established by taking the Dwarf Big Head 567 oil sunflower seeds as the object. The three-axis dimensions (maximum length, maximum width, and maximum thickness) of the oil sunflower seeds were measured using a 111N-101-40 absolute origin digital display caliper (accuracy 0.01 mm), and the results of the measurements are listed in Table 1. The oil sunflower seeds with length, width, and height close to the average were selected, and the GD-3DScan three-dimensional (3D) scanner was used to obtain the 3D coordinates of the outer surface of the oil sunflower seeds and generate the point cloud data using the inverse modeling technique<sup>[16]</sup>. Point cloud data were merged and sharpened using Geomagic Studio and GOM Inspect software, respectively. A 3D model of oil sunflower seeds was obtained and imported into EDEM software for particle filling<sup>[17,18]</sup>.

**Table 1 Three-dimensional geometric size of dwarf big head 567 oil sunflower seeds**

Three-axis dimensions	Distribution of sizes		Average value/mm	Standard deviation
	Range of sizes/mm	Percentage/%		
Length	11.77-12.70	7.68	13.36	0.435
	12.72-14.05	89.37		
	14.06-14.68	2.95		
Width	4.89-6.14	3.94	6.94	0.420
	6.15-7.59	93.11		
	7.62-8.13	2.95		
Thickness	3.17-3.59	0.98	4.63	0.405
	3.71-5.33	95.87		
	5.35-5.77	3.15		

EDEM uses the combined ball method for the particle filling of 3D models, which has been widely used in the simulation analysis of agricultural materials such as peanuts, wheat, maize, and soybeans<sup>[19,20]</sup>. When the particles are filled, the smaller the particles filled on the surface of the material, the smaller the surface grooves of the model obtained. That is, the smoothness is better and closer to the real characteristics of the agricultural material. However, the smaller the filled particles are, the larger the amount of filled particles is, resulting in excessive simulation calculations and low simulation efficiency. When using EDEM software for particle filling, different smoothing values can be set to obtain a discrete element model filled with a different number of particles. The 3D model of oil sunflower seeds established using 3D scanning was imported into EDEM software as a template. The smoothing value was set to 2, 5, 8, 11, 14, and 17 to obtain six discrete element models of oil sunflower seeds filled with different numbers of particles, as presented in Figure 1.

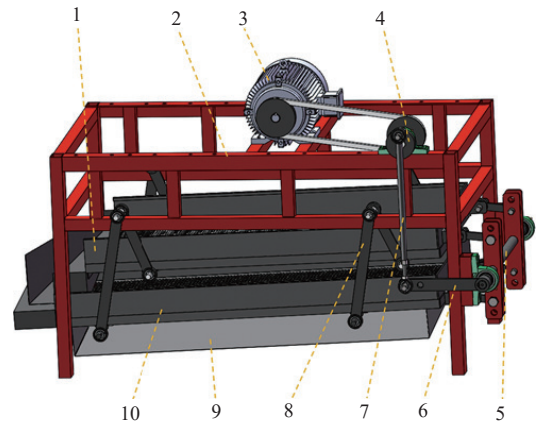
### 2.2 Vibrating screen model and contact model

#### 2.2.1 Vibrating screen model

The pendulum-type vibrating screen has advantages such as simple structure, stable work, and no additional excitation source.

Its screen surface motion trajectory is a complex two-dimensional plane motion, which has good screening performance<sup>[10,13]</sup>. Therefore, the pendulum-type vibrating screen is widely used in combined harvester and threshing equipment. In this paper, a pendulum-type double-deck vibrating screen for screening oil sunflower debris is designed, as presented in Figure 2. The upper vibrating screen has a length of 1200 mm, a width of 600 mm, and a height of 110 mm, whereas the lower vibrating screen has a length of 1300 mm, a width of 700 mm, and a height of 110 mm. The motor drives the eccentric wheel to rotate, and the eccentric wheel drives the linkage mechanism to drive the oscillating assembly to achieve cyclic twisting motion. The oscillating arm is welded to the oscillating assembly, and the upper and lower vibrating screens are connected to the upper and lower ends of the oscillating arm, respectively. The upper and lower two layers of vibrating screen are placed parallel to each other and suspended on the frame by the rocker. The initial vibration phase angle of the two screens differs by 180°, so that the upper and lower two layers of vibrating screens always keep the movement in opposite directions, thus reducing the degree of shaking of the whole machine and keeping the machine running smoothly. When working, the pendulum-type double-deck vibrating screen makes the oil sunflower seeds slide forward rapidly in the state of throwing motion, which can facilitate the fast separation of oil sunflower seeds on the screen surface and increase the chance of passing through the screen holes.

forces and moments between the oil sunflower seeds and the vibrating screen and transmits them back to RecurDyn. EDEM coupled with RecurDyn analysis can identify the interaction between the vibrating screen and the oil sunflower seeds and can reflect the kinetic behavior of the particles more realistically. To facilitate the simulation processing, a simplified simulation model of the double-deck vibrating screen is established<sup>[6,13,21-23]</sup>, as presented in Figure 3.



1. Upper vibrating screen 2. Frame 3. Motor 4. Eccentric wheel 5. Swing assembly 6. Swing arm 7. Link mechanism 8. Rocker 9. Soil guide box 10. Lower vibrating screen

Figure 2 Pendulum-type double-deck vibrating screen

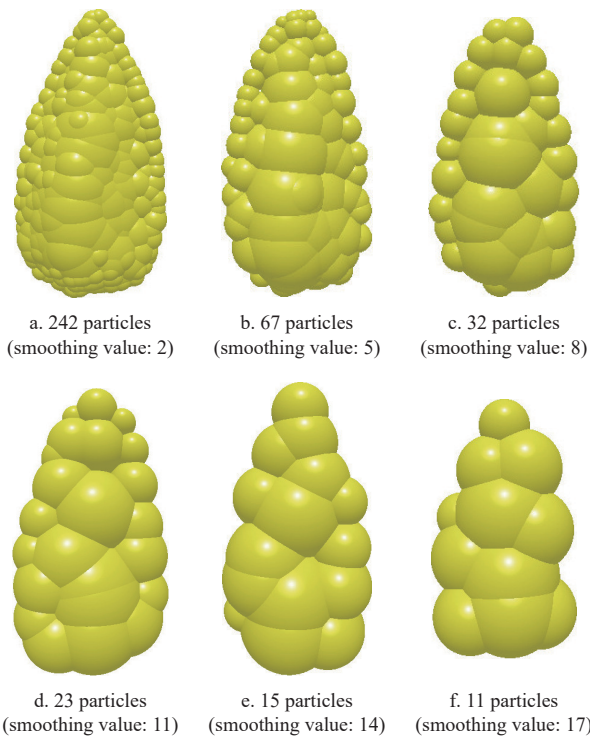


Figure 1 Oil sunflower seed discrete element models

The behavior of oil sunflower seeds passing through the screen holes mainly occurs in the upper vibrating screen; hence, this paper analyzes the behavior of oil sunflower seeds passing through the screen holes for the upper vibrating screen. Only basic motion behaviors can be simulated in an EDEM environment; complex motion behaviors must be identified using coupling techniques. Therefore, this paper uses EDEM and RecurDyn software for coupling simulation analysis. The motion of the vibrating screen is simulated in RecurDyn software, and then the dynamics information of the vibrating screen is passed to EDEM. EDEM calculates the

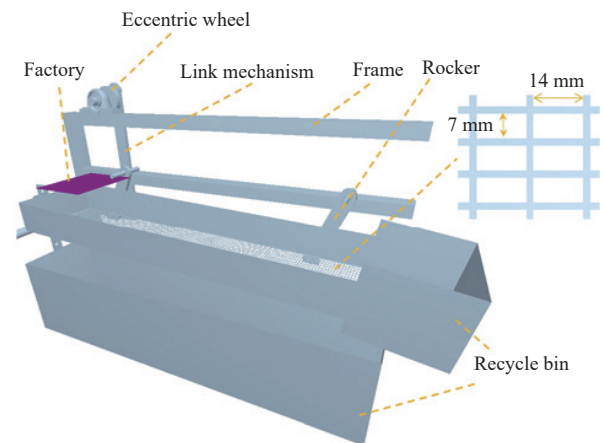


Figure 3 Simplified simulation model of vibrating screen

### 2.2.2 Contact model selection

There was no adhesion between the oil sunflower seeds and no additional resistance when the particles moved on the vibrating screen. Therefore, the simulation analysis of the oil sunflower seed motion process was based on the Hertz-Mindlin no-slip contact model<sup>[24-26]</sup>. In this study, a multi-sphere cluster combination filling method was used to fill the oil sunflower seeds. When particle contact occurs, the amount of overlap is generated at the contact point between the particle and the particle or the contact material<sup>[27]</sup>. According to Newton's second law of motion, the cross-folded quantities are introduced into the process of calculating the contact force, and the contact force and displacements between the particles are determined using the contact model.

The relationship of normal force  $F_n$  and normal damping force  $F_n^d$  between oil sunflower seeds and the contact material should satisfy Equation (1). The relationship equation of tangential force  $F_t$  and tangential damping force  $F_t^d$  should satisfy Equation (2). The equations of translational and rotational motion of the particles

should satisfy Equations (3) and (4). Equations (1)-(4) are calculated as follows:

$$\begin{cases} F_n = \frac{4}{3} E^* (R^*)^{1/2} \alpha^{3/2} \\ F_n^d = -2 \sqrt{\frac{5}{6}} \beta \sqrt{S_n m^* v_n^{rel}} \end{cases} \quad (1)$$

$$\begin{cases} F_t = -S_t \delta \\ F_t^d = -2 \sqrt{\frac{5}{6}} \beta \sqrt{S_t m^* v_t^{rel}} \end{cases} \quad (2)$$

$$m_i \frac{dv_i}{dt} = \sum_{j=1}^{n_i} (F_{n,ij} + F_{t,ij} + F_{n,ij}^d + F_{t,ij}^d) + m_i g \quad (3)$$

$$I_i \frac{d\omega_i}{dt} = \sum_{j=1}^{n_i} (T_{t,ij} + T_{r,ij}) \quad (4)$$

where,  $F_n$ ,  $F_n^d$ ,  $F_t$ , and  $F_t^d$  are normal force, normal damping force, tangential force, and tangential damping force, respectively;  $E^*$  is the equivalent elastic modulus;  $R^*$  is the equivalent radius of the model particles;  $\alpha$  is the normal overlap;  $\beta$  is the damping ratios;  $S_n$  is the normal stiffness;  $m^*$  is the equivalent mass;  $v_n^{rel}$  is the relative normal component of velocity;  $S_t$  is the tangential stiffness;  $\delta$  is the tangential overlap;  $v_t^{rel}$  is the tangential relative velocity;  $n_i$  is the number of particles in contact with particle  $i$ ;  $m_i$ ,  $I_i$ ,  $\omega_i$ , and  $v_i$  are the mass, moment of inertia, angular velocity, and linear velocity vectors of particle  $i$ , respectively;  $g$  is gravitational acceleration;  $T_{t,ij}$  is the moment caused by tangential force;  $T_{r,ij}$  is the moment caused by rolling friction.

**2.3 Force analysis of oil sunflower seeds and motion analysis of screen surface**

The motion state of oil sunflower seeds is closely related to the force condition, and its motion form relative to the screen surface mainly has four types: forward slip, backward slip, throwing off, and stationary. Take any one oil sunflower seed on the screen surface as the research object; the force analysis when the oil sunflower seed is in contact with the screen surface is shown in Figure 4.

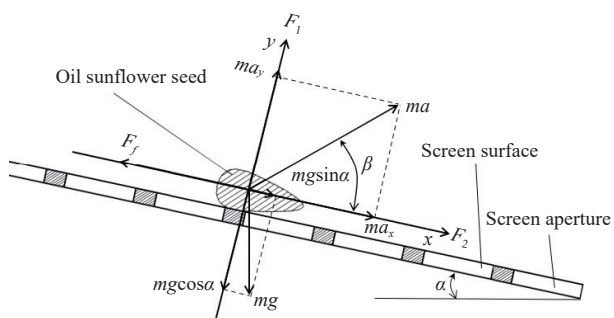


Figure 4 Force analysis of oil sunflower seeds.

The motion state of oil sunflower seeds on the screen surface is directly related to the combined force  $F_1$  of oil sunflower seeds along the vertical screen surface direction and the combined force  $F_2$  of oil sunflower seeds along the parallel screen surface direction. When  $F_1 > 0$ , oil sunflower seeds reach the basic conditions of throwing phenomenon. When  $F_1 \leq 0$  and  $F_2 > 0$ , oil sunflower seeds slide forward along the screen. When  $F_1 \leq 0$  and  $F_2 < 0$ , oil sunflower seeds slide backward along the screen. When  $F_1 = 0$  and  $F_2 = 0$ , oil sunflower seeds are balanced by forces on the screen surface and are in a relative resting state or uniform sliding motion.

$$F_1 = m a \sin \beta - m g \cos \alpha \quad (5)$$

$$F_2 = m a \cos \beta + m g \sin \alpha - F_f \quad (6)$$

$$\begin{cases} k_v = \frac{A \omega^2 \sin \beta}{g \cos \alpha} = k' \frac{\sin \beta}{\cos \alpha} \geq 1 \\ k' = \frac{A \omega^2}{g} \end{cases} \quad (7)$$

where,  $F_1$  is the resultant force of oil sunflower seeds up along the vertical screen surface, N;  $F_2$  is the resultant force of oil sunflower seeds forward along the parallel screen surface, N;  $m$  is the mass of oil sunflower seeds, g;  $\alpha$  is the inclination angle of the screen surface, ( $^\circ$ );  $\beta$  is the throwing angle, ( $^\circ$ );  $g$  is the acceleration of gravity, m/s<sup>2</sup>;  $F_f$  is the friction between the oil sunflower seeds and the screen surface, N;  $a$  is the acceleration of the oil sunflower seeds, m/s<sup>2</sup>;  $A$  is the amplitude of the screen surface, m;  $\omega$  is the angular velocity of the screen surface, rad/s;  $k_v$  is the throwing index of the vibrating screen;  $k'$  is the vibration intensity index of the vibrating screen.

From Equation (5), it is clear that  $F_1=0$  is the critical condition for the occurrence of the throwing phenomenon in oil sunflower seeds. Assuming that the maximum amplitude of the vibrating screen is  $A$ , the acceleration of the whole screening process is less than  $A\omega^2$ . The maximum acceleration of the vibrating screen is substituted into Equation (5) to obtain Equation (7). From Equation (7), it can be noted that whether the oil sunflower seeds are thrown or not can be determined by analyzing the size of  $k_v$ . When  $k_v > 1$ , the resultant force of the oil sunflower seeds is perpendicular to the screen surface upward, and the throwing phenomenon can occur. When  $k_v < 1$ , the resultant force of the oil sunflower seeds is perpendicular to the screen surface downward, and the throwing phenomenon cannot occur. The group of oil sunflower seeds under the action of the screen surface has forward throwing movement, which is conducive to the forward transportation of oil sunflower seeds along the screen surface. In addition, the aforementioned phenomenon can increase the degree of dispersion of oil sunflower seeds in the conveying process, increasing the chance of passing through the screen holes.

The simplified model of the vibrating screen is imported into RecurDyn software, and the corresponding kinematic pairs and driving forces are added. The simulation time is set to 0.5 s, and the number of steps is set to 100 to start the motion simulation. The motion trajectory of three points is plotted at the exit of the screen surface ( $A$ ), the center of mass of the screen surface ( $B$ ), and the feed of the screen surface ( $C$ ). In addition, the three motion trajectories are translated to the endpoint overlap to obtain the motion trajectory comparison curve, as presented in Figure 5.

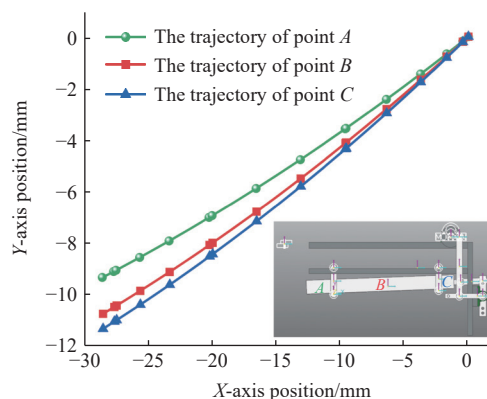


Figure 5 Movement trajectory comparison curve

From Figure 5, it can be noted that the displacement changes of points A, B, and C along the horizontal screen surface direction (x-axis) are all 28.7 mm, and the displacement changes along the vertical screen surface direction (y-axis) are all between 0 and 11.32 mm. The displacement is ranked from the largest to smallest

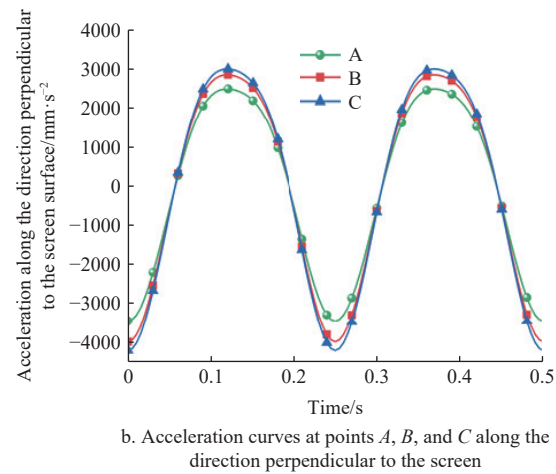
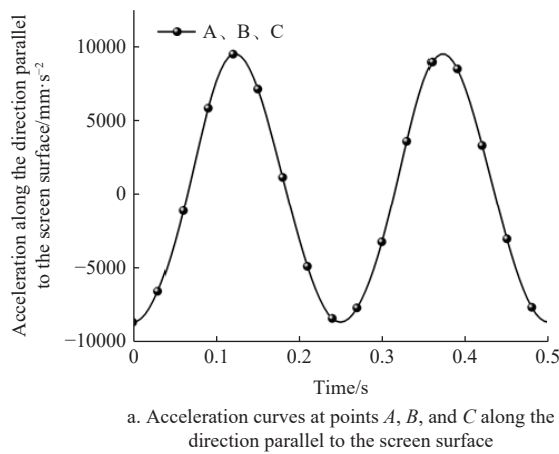


Figure 6 Acceleration change curves at points A, B, and C

As can be noted from Figure 6, the acceleration of the vibrating screen in both the parallel screen surface direction and the vertical screen surface direction is a periodic variation that is approximately sinusoidal. It can be noted from Figure 6a that the acceleration changes of points A, B, and C along the direction parallel to the screen surface are consistent. As can be noted from Figure 6b, the average acceleration of points A, B, and C along the direction of the vertical screen surface is ordered from the largest to smallest as C, B, and A. Therefore, the force on the oil sunflower seeds at points A, B, and C along the vertical screen surface is ranked from the largest to smallest as C, B, and A. This phenomenon is conducive to the throwing phenomenon of oil sunflower seeds at the feed. Therefore, the average acceleration of the three points along the parallel screen surface direction is much greater than that along the vertical screen surface direction. It indicates that the oil sunflower seeds have a throwing tendency when moving on the screen surface. In addition, the degree of throwing from the feed place to the exit place gradually becomes smaller. This process is conducive to the forward movement of oil sunflower seeds and can effectively prevent the accumulation of oil sunflower seeds at the inlet from blocking.

2.4 Test method

This research uses the stacking test to compare the effect of particle filling amount of discrete element model of oil sunflower seeds on the simulation effect. Simulation parameters are presented in Table 2<sup>[28]</sup>. The stacking test (Figure 7) was performed using the cylinder lifting method, and the angle of repose  $\theta$  for the physical stacking test of oil sunflower seeds was obtained as 48.858°. In this study, a cylinder lifting simulation was performed using the same configuration of a computer with the same method for a discrete element model of oil sunflower seeds with different particle fillings. Each simulation test was repeated five times, and the time used for the simulation was recorded. Computer Configuration: CPU: Intel(R) Core(TM) i9-10900X CPU@3.70 GHz, Running Memory: 64 GB, Graphics Card: NVIDIA GeForce RTX 3090. The simulation settings are uniformly set as follows: the Rayleigh time step is 10%, the target save interval is 0.01 s, the cell size is 3R, and the dynamic computational domain is turned on. When the velocities of all particles are less than 0.001 m/s, the oil sunflower seed pile is considered to have reached a stable state on the slope.

as C, B, and A, indicating that the closer the feed place, the more significant the displacement change. The acceleration of the screen surface movement can reflect the force of the oil sunflower seeds on the screen surface; hence, the acceleration of points A, B, and C was analyzed. The acceleration variation curve is presented in Figure 6.

The edge contour of the angle of repose is extracted using MATLAB, and the extracted edge contour is imported into Origin software to obtain the slope of the edge contour and transform it into angle  $\beta$ . The relative error Y between the angle of repose of the simulation test and the angle of repose of the physical test is calculated, as shown in Equation (8):

$$Y = \frac{|\beta - \theta|}{\theta} \tag{8}$$

Table 2 Simulation parameters

Symbol	Parameters	Value
$X_1$	Poisson's ratio of oil sunflower seeds	0.413
$X_2$	Density of oil sunflower seeds/kg·m <sup>-3</sup>	849.4
$X_3$	Shear modulus of oil sunflower seeds/Pa	1.0782e+08
$X_4$	Coefficient of restitution between oil sunflower seeds	0.5
$X_5$	Coefficient of static friction between oil sunflower seeds	0.41
$X_6$	Coefficient of rolling friction between oil sunflower seeds	0.05
$X_7$	Coefficient of restitution between oil sunflower seeds and steel plates	0.35
$X_8$	Coefficient of static friction between oil sunflower seeds and steel plates	0.423
$X_9$	Coefficient of rolling friction between oil sunflower seeds and steel plates	0.125



1. HY-0580 universal material tensile and compression testing machine  
 2. Computer 3. Oil sunflower seed 4. Camera 5. Stainless steel round table  
 6. Stainless steel cylinder

Figure 7 Physical stacking test of oil sunflower seeds

The screening simulation process of oil sunflower seeds is presented in Figure 8, and the process is divided into three main

stages. When the screening simulation starts, the oil sunflower seeds generated by the particle factory are continuously fed from the feed end, and the oil sunflower seeds come into contact with the screen surface and create a brief accumulation phenomenon. The oil sunflower seeds start to disperse and move forward along the horizontal screen surface under the action of vibration, and this process is the initial stage of screening, as presented in Figure 9a. When the total mass of oil sunflower seeds on the screen surface fluctuates slightly above and below a certain level value, the screening steady-state stage is reached, as presented in Figure 9b. When the feeding was stopped, the oil sunflower seeds on the screen surface continued to exhibit screen penetration behavior. The mass of oil sunflower seeds on the screen surface gradually decreases until the screening is completed, and this process is the end stage of screening, as presented in Figure 9c. In the whole screening process, most of the oil sunflower seeds pass through the screen surface and move under the screen, and a small part of the oil sunflower seeds that cannot pass through the screen moves forward along the screen surface and finally discharges into the collection box, which becomes the screening loss. The screening percentage is the percentage of the mass of oil sunflower seeds that have been sieved divided by the total mass of oil sunflower seeds, which is an important index to evaluate the performance of the screening device, and the screening percentage is calculated, as shown in Equation (9). The screening percentage of the steady-state stage of screening is relatively stable; hence, the screening percentage of the steady-state stage of screening was analyzed in this study.

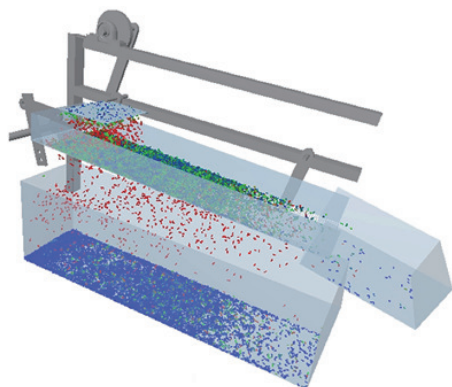


Figure 8 Simulation test of the screening process of oil sunflower seeds

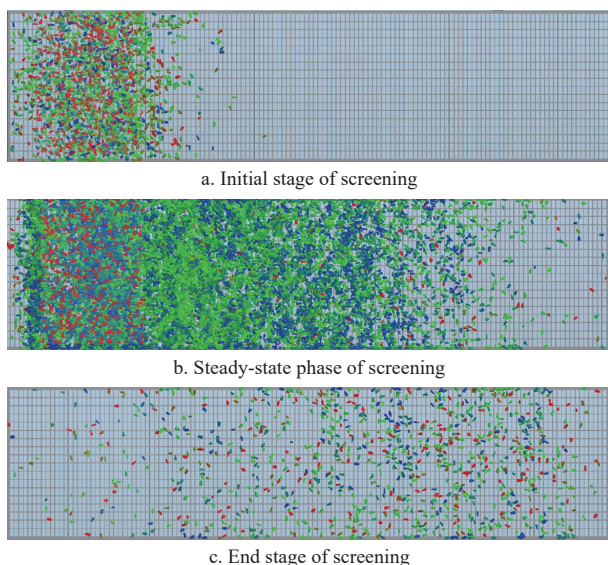


Figure 9 Distribution of oil sunflower seeds on the screen surface

$$\eta = \frac{m_1}{m_1 + m_2 + m_3} \times 100\% \tag{9}$$

where,  $\eta$  is the screening percentage of oil sunflower seeds, %;  $m_1$  is the mass of oil sunflower seeds passing through the screen holes, g;  $m_2$  is the mass of oil sunflower seeds on the screen surface, g;  $m_3$  is the mass of oil sunflower seeds lost from the screen surface outlet, g.

The number of parabolic motions of oil sunflower seeds on the screen surface is influenced by the working parameters of the vibrating screen. In the screening stabilization stage, the oil sunflower seeds on the screen surface repeat the process of throwing off the screen surface and returning to the screen surface. When most of the particles are thrown off, the total pressure of oil sunflower seeds on the screen surface is minimized. When most of the particles collide with the screen surface, the total pressure of oil sunflower seeds on the screen surface is the largest. Therefore, the number of parabolic motions of oil sunflower seeds on the screen surface is related to the force on the screen surface. In this study, the number of times that the maximum value of pressure on the sieve surface occurred was approximated as the number of parabolic motions of oil sunflower seeds on the screen surface.

The feeding speed, vibration frequency, and screen surface inclination angle were selected as the test factors. A single-factor test was used to investigate the effects of each test factor on the screening percentage and the number of parabolic motions of oil sunflower seeds. The Box-Behnken test was designed to analyze the effect of each test factor on the screening percentage of oil sunflower seeds and to optimize the working parameters of the vibrating screen. According to the pretest and simulation pretest of this paper, the optimal feeding speed range is 0.3-0.9 kg/s, the optimal vibration frequency range is 2-7 Hz, and the optimal screen surface inclination range is 0°-6°.

### 3 Results and discussion

#### 3.1 Effect of particle filling amount of discrete element model of oil sunflower seeds on simulation effect

Discrete element models of oil sunflower seeds with different particle fillings were subjected to cylinder lifting simulation tests, and the results are presented in Table 3. The results indicate that the simulation time tends to increase substantially with the increase of particle filling, and the relative error of the angle of repose tends to decrease. The relative error between the angle of repose of the simulated test and the angle of repose of the physical test was in the range of 0.16%-0.36% for different particle filling amounts, and the errors were within reasonable limits. When the particle filling amount was between 11 and 23, the simulation time changed less. When the particle filling amounts were 32, 67, and 242, the simulation times were 8.5, 58, and 187 times the simulation time when the particle filling amount was 23, respectively. The simulation time appeared to increase sharply, and the computational efficiency was critically decreased. To control the relative error within a reasonable range and increase the simulation efficiency, 23 particle-filled oil sunflower seed models were formulated for subsequent simulation experiments.

#### 3.2 Analysis of single-factor experiment results

The patterns of the effects of the test factors on the screening percentage and the number of parabolic motions of oil sunflower seeds are presented in Figure 10.

The feeding speeds selected were 0.3, 0.4, 0.5, 0.6, 0.7, 0.8, and 0.9 kg/s. The vibration frequency and screen surface inclination were 4 Hz and 2°, respectively, for the tests. The effects of feeding

speed on the screening percentage and the number of parabolic motions of oil sunflower seeds are presented in Figure 10a. The results indicated that with the increase in feeding speed, the screening percentage decreased from 99.358% to 97.429%, which was a year-on-year decrease of 1.941%, showing a continuous decreasing trend. The main reason for the decrease in the screening percentage is that when the feeding speed increased, the thickness of oil sunflower seeds in the direction of the vertical screen surface increased, which decreased the chance of contact between oil sunflower seeds and the screen surface. The number of parabolic motions made by oil sunflower seeds was stable in the range of 37-40 times. Moreover, the number of parabolic motions made by the oil sunflower seeds did not change significantly with the increase in feeding speed; hence, the effect of feeding speed change on the number of parabolic motions made by the particles was small. When the feeding speed was 0.3 kg/s, the oil sunflower seeds had

the highest screening percentage but low working efficiency, which affected the processing capacity of the vibrating screen. To ensure the efficiency of the vibrating screen, the proposed feeding speed range is 0.4-0.6 kg/s.

**Table 3 Experimental results of model oil sunflower seeds with different particle filling amounts**

Case	Smoothin g value	Number of particles	Angle of repose of the simulation test $\beta/(\circ)$	Relative error Y/%	Simulation time/h
1	2	242	48.936	0.16	187
2	5	67	48.976	0.24	58
3	8	32	48.741	0.27	8.50
4	11	23	48.714	0.29	1
5	14	15	49.029	0.35	0.87
6	17	11	49.034	0.36	0.57

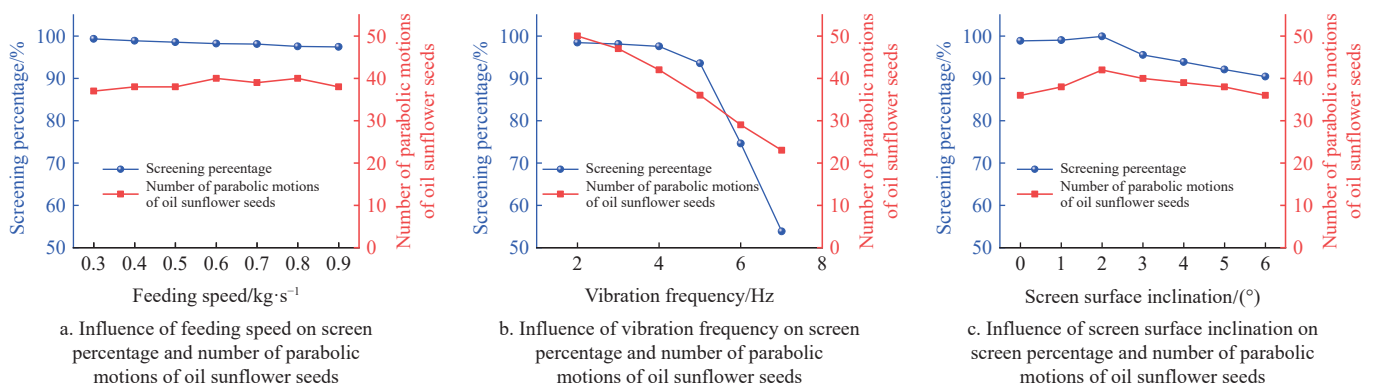


Figure 10 Analysis of single-factor experiments results

The Vibration frequencies of 2, 3, 4, 5, 6, and 7 Hz were selected. The feeding speed and screen surface inclination were 0.5 kg/s and 2°, respectively, for the tests. The influence of the law of vibration frequency on the screening percentage and the number of parabolic motions of oil sunflower seeds was investigated, as presented in Figure 10b. The curve of the average velocity change of particles in the x-axis direction at different frequencies is presented in Figure 11. When the curve was below the velocity reference line, the oil sunflower seeds moved toward the exit of the vibrating screen. When the curve was above the velocity reference line, the oil sunflower seeds moved in the opposite direction of the vibrating screen outlet. When the average velocity change curve in the x-axis direction fluctuated above and below the velocity reference line, the movement of the oil sunflower seeds indicated alternating forwarding and backward reciprocation. The more the curve was distributed below the velocity reference line, the greater the degree of forwarding advance of the sunflower seeds. As presented in Figure 11, with the increase of vibration frequency, the amplitude of motion of oil sunflower seeds along the x-axis direction increased, and the curve below the reference line of distribution velocity gradually increased. The aforementioned phenomena indicated that the degree of forwarding transport of oil sunflower seeds along the screen surface was enhanced. When the vibration frequency was 7 Hz, the average velocity variation curve in the x-axis direction was below the velocity reference line. The oil sunflower seeds exhibited no reciprocal movement phenomenon and showed the phenomenon of forward rapid transport.

As can be noted from Figure 10b, when the vibration frequency was variable, the screening percentage of oil sunflower seeds was positively correlated with the number of parabolic motions. The

number of parabolic motions and screening percentage of oil sunflower seeds continued to decrease with the increase in vibration frequency. The number of parabolic motions decreased from 50 to 23, which was a year-on-year decrease of 54%. The screening percentage decreased from 98.462% to 53.846%, which was a year-on-year decrease of 45.313%. In order to further analyze the effect of frequency on the average velocity of the particles in the X direction, feature spectrum analysis of the vibration frequency was carried out<sup>[29]</sup>. The results are shown in Figure 12. As can be seen from Figure 12, as the frequency increases, the amplitude in the frequency domain analysis first increases and then decreases, and an inflection point occurs at 5 Hz. Therefore, this paper comprehensively analyzes the influence curve of vibration frequency on the movement of oil sunflower seeds and sieve penetration rate, as shown in Figure 13. As presented in Figure 13, when the vibration frequency increased, the rate of motion of oil sunflower seeds along the negative direction of the x-axis increased from 1.354 to 132.459 m/s, which was a large increase. When the vibration frequency increased in the range of 0-4 Hz, the rate of motion of oil sunflower seeds along the negative direction of the x-axis increased from 1.354 to 31.713 m/s, and the screening percentage of oil sunflower seeds decreased from 98.462% to 97.558%, with a smaller year-on-year decrease of 0.875%. When the vibration frequency was increased in the range of 5-7 Hz, the rate of motion of oil sunflower seeds along the negative direction of the x-axis increased from 56.5147 to 132.4590 m/s, and the screening percentage of oil sunflower seeds decreased from 93.543% to 53.846%, which was a significant year-on-year decrease of 42.437%. Taken together, when the vibration frequency increased in the range of 0-4 Hz, the screening percentage of oil

sunflower seeds was decreased to a lesser extent, but the efficiency of the vibrating screen was significantly improved. When the vibration frequency increased in the range of 5-7 Hz, the reduction of the screening percentage of oil sunflower seeds was greater, but the increase in the efficiency of the vibrating screen was relatively small. To ensure the screening percentage, while considering the processing efficiency of the vibrating screen, the selected vibration frequency range is 3-5 Hz.

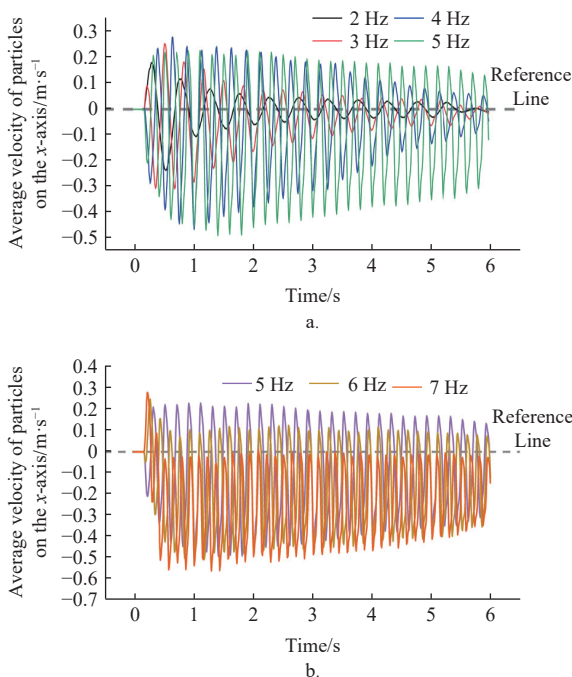


Figure 11 Variation curve of the average velocity of particles on the x-axis at different frequencies

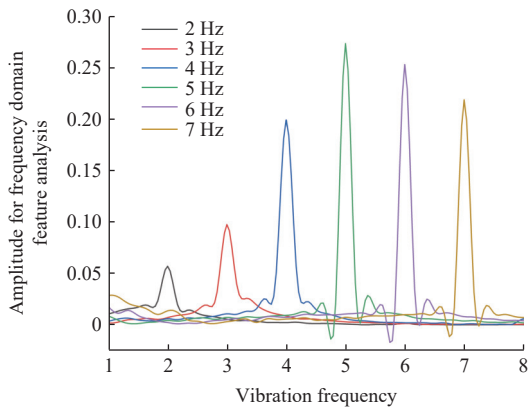


Figure 12 Feature spectrum analyses of vibration frequencies

The screen surface inclinations selected were 0°, 1°, 2°, 3°, 4°, 5°, and 6°. The feeding speed and vibration frequency were 0.5 kg/s and 4 Hz, respectively, for the tests. Figure 10c displays the pattern of the effect of screen surface inclination on the screening percentage and number of parabolic motions of oil sunflower seeds. The results indicated that when the screen surface inclination was from 0° to 2°, with the increase of screen surface inclination, the screening percentage of oil sunflower seeds and the number of parabolic motions of oil sunflower seed groups both exhibited an increasing trend. The screening percentage of oil sunflower seeds increased from 98.870% to 99.970%, which was a year-on-year increase of 1.113%. When the screen surface inclination was from 2° to 6°, with the increase of screen surface inclination, the

screening percentage of oil sunflower seeds and the number of parabolic motions of oil sunflower seed groups both indicated a decreasing trend. The screening percentage of oil sunflower seeds decreased from 95.540% to 90.460%, which was a year-on-year decrease of 5.317%. To ensure the screening percentage, the proposed screen surface inclination range is 1°-3°.

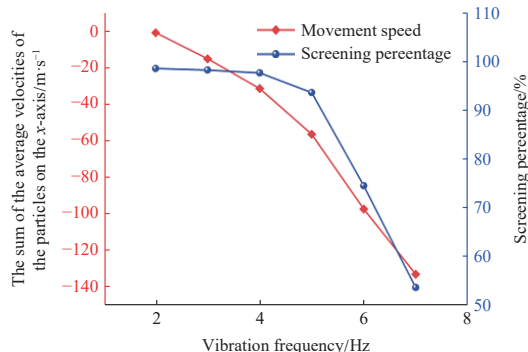


Figure 13 Effects of vibration frequency on the movement and screening percentage of oil sunflower seeds

### 3.3 Analysis of multifactor experiment results

The factor levels of the response surface tests were set according to the range of each factor in the results of the single-factor test analysis, as presented in Table 4. The Box-Behnken test was designed using Design-Expert 10.0.7 software. Screening tests were performed on 15 groups of factors in different level combinations, three of which were repeated at the central level. This experiment analyzed the influence of the law of feeding speed, vibration frequency, and screen surface inclination on the screening percentage of oil sunflower seeds and optimized the working parameters of the vibrating screen. Table 5 lists the Box-Behnken experimental design scheme and results. Multiple regression fitting analysis was performed on the test data in Table 5 using Design-Expert 10.0.7 software to obtain the ANOVA results, as presented in Table 5. The regression model of the screening percentage of oil sunflower seeds with the coded values of each test factor was established as presented in Equation (10).

$$R_1 = 92.37 - 11.42B_1 - 1.9C_1 - 3.01B_1C_1 - 4.87B_1^2 \quad (10)$$

As presented in Table 6, the significance test value of the  $R_1$  regression model is  $P = 0.0006$ , that of the lack of fit term is  $P = 0.3198$ , and the coefficient of determination  $R_2 = 0.9839$ . The regression model is significant, the lack of fit term is not significant, and the coefficient of determination is close to 1, indicating a good fit of the  $R_1$  regression model. The smaller the coefficient of variation ( $CV$ ), the more reliable the test data are. The coefficient of variation ( $CV$ ) of the  $R_1$  regression model was 2.22%, indicating that the test data are reliable<sup>[28,30,31]</sup>. The comparison between the predicted and tested values of the  $R_1$  regression model is presented in Figure 14. The Adep precision of the regression model was 17.714, which is much greater than 4, and the test values were evenly distributed around the prediction curve, indicating that the regression model could predict the screening percentage of oil sunflower seeds better. From Table 5, the effects on the screening percentage of oil sunflower seeds can be noted:  $B_1$  and  $B_1^2$  were highly significant,  $C_1$  and  $B_1C_1$  were significant, and the descending order of significance of the effects was  $B_1$ ,  $B_1^2$ ,  $B_1C_1$  and  $C_1$ . The interaction between the test factors and the screening percentage of oil sunflower seeds has a quadratic nonlinear relationship. The interaction of vibration frequency and screen inclination had a

significant effect on the screening percentage of oil sunflower seeds, whereas the remaining interaction terms did not have a significant effect on the screening percentage of oil sunflower seeds. The response surface of the relationship between the screening percentage of oil sunflower seeds and each test factor is presented in Figure 15.

**Table 4 Coding table of test factor level**

Code	Feeding speed/kg·s <sup>-1</sup>	Vibration frequency/Hz	Screen surface inclination/(°)
-1	0.4	3	1
0	0.5	4	2
1	0.6	5	3

**Table 5 Box-Behnken test design and results**

Case	A <sub>1</sub>	B <sub>1</sub>	C <sub>1</sub>	Screening percentage of oil sunflower seeds R <sub>1</sub> /%
1	-1	-1	0	99.258
2	0	1	-1	83.755
3	0	-1	1	98.989
4	1	1	0	73.003
5	1	0	1	90.930
6	1	-1	0	98.272
7	0	0	0	91.996
8	-1	0	-1	94.646
9	1	0	-1	92.121
10	0	0	0	90.442
11	-1	0	1	92.978
12	0	1	1	71.541
13	0	-1	-1	99.151
14	0	0	0	93.446
15	-1	1	0	75.996

**Table 6 Box-Behnken experimental regression model analysis of variance**

Source	Sum of squares	Degree of freedom	Mean square	F-value	p-value
Model	1214.57	9	134.95	33.87	0.0006**
A <sub>1</sub>	9.14	1	9.14	2.29	0.1903
B <sub>1</sub>	1043.68	1	1043.68	261.93	<0.0001**
C <sub>1</sub>	29.02	1	29.02	7.28	0.0429*
A <sub>1</sub> B <sub>1</sub>	1.01	1	1.01	0.25	0.6365
A <sub>1</sub> C <sub>1</sub>	0.057	1	0.057	0.014	0.9094
B <sub>1</sub> C <sub>1</sub>	36.32	1	36.32	9.11	0.0295*
A <sub>1</sub> <sup>2</sup>	0.96	1	0.96	0.24	0.6444
B <sub>1</sub> <sup>2</sup>	85.75	1	85.75	21.52	0.0056**
C <sub>1</sub> <sup>2</sup>	5.47	1	5.47	1.37	0.2942
Residual	19.92	5	3.98	--	--
Lack of fit	15.41	3	5.14	2.28	0.3198
Pure error	4.51	2	2.26	--	--

Note: CV = 2.22%, R<sup>2</sup> = 0.9839, and accuracy = 17.714.

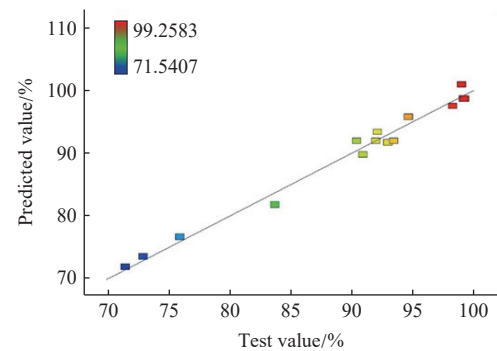


Figure 14 Regression model predicted values versus experimental values

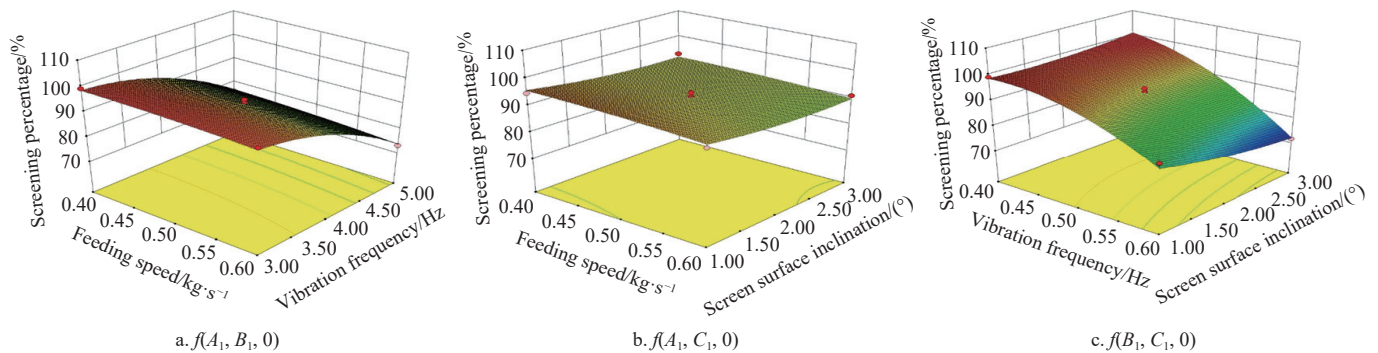


Figure 15 Response surface for the screening percentage of oil sunflower seeds

$$\begin{cases} \max R_1(ABC) \\ 0.4 \leq A \leq 0.6 \\ 3 \leq B \leq 5 \\ 1 \leq C \leq 3 \end{cases} \quad (11)$$

Based on the aforementioned experimental results, with the optimization objective of increasing the screening percentage of oil sunflower seeds, Design-Expert 10.0.7 was used to establish the objective function and the factor constraints as presented in Equation (11). According to Equation (11), the regression model is solved using the optimization numerical optimization module. The results indicated that when the feeding speed was 0.45 kg/s, the vibration frequency was 3 Hz, and the screen surface inclination was 2.7°, the oil sunflower seeds had a high screening percentage, which could reach 99.92% at that time.

### 4 Conclusions

1) With the combination of the inverse modeling technique and EDEM software, six discrete element models of oil sunflower seeds filled with different amounts of particles were established. The lifting test results of cylinders indicated that the discrete element model of oil sunflower seeds filled with 23 particles had better simulation test results.

2) In this study, a pendulum-type double-deck vibrating screen was designed for the screening of oil sunflower debris. The force state of oil sunflower seeds on the screen surface was analyzed by taking oil sunflower seeds on the screen surface as the object. The results indicate that the motion state of oil sunflower seeds on the screen surface is directly related to the combined force of oil sunflower seeds along the vertical screen surface direction and the

combined force of oil sunflower seeds along the parallel screen surface direction. RecurDyn software was used to establish a vibrating screen dynamic model, and a point was selected at the exit of the screen surface, at the center of mass of the screen surface, and at the feed of the screen surface to analyze the motion state of the screen surface. The results indicate that the motion of the screen surface is favorable to the forward throwing of the oil sunflower seeds, and the accumulation of oil sunflower seeds at the feed can be avoided.

3) The single-factor test was used to investigate the effect of each test factor on the screening percentage and the number of parabolic motions of oil sunflower seeds. The results indicate that the order of influence on the screening percentage of oil sunflower seeds and the number of parabolic motions of the particles is in descending order: vibration frequency, screen surface inclination, and feeding speed. The number of parabolic motions and screening percentage of oil sunflower seeds continued to decrease with the increase in vibration frequency. With the increase in vibration frequency, the number of parabolic motions decreased from 50 to 23, which was 54% lower than that of the same period last year; with the increase in vibration frequency, the screening percentage decreased from 98.462% to 53.846%, which was 45.313% lower than that of the same period last year.

4) The results of the Box-Behnken test were analyzed with ANOVA using Design-Expert software, and a regression model for the screening percentage of oil sunflower seeds was developed. Optimal calculation was performed to improve the screening percentage, and the optimal combination of test factors was found to be a feeding speed of 0.45 kg/s, a vibration frequency of 3 Hz, and a screen surface inclination of 2.7°. The screening simulation test was conducted with the optimal combination of parameters, and the screening percentage of oil sunflower seeds was 99.92%.

## Acknowledgments

The authors acknowledge that this work was financially supported by Hebei Agriculture Research System HBCT2024 040207. The authors also thank their colleagues from the College of Engineering, Nanjing Agricultural University, and the School of Mechanical and Electrical Engineering, Hebei Agricultural University, for their help during the experiments. We thank LetPub ([www.letpub.com](http://www.letpub.com)) for its linguistic assistance during the preparation of this manuscript.

## [References]

- [1] Jin W, Ding Y C, Bai S H, Zhang X J, Yan J S, Zhou X C. Design and experiments of the reel board header device for an oil sunflower harvester. *Transactions of the CSAE*, 2021, 37(3): 27–36. (in Chinese)
- [2] Liu Y, Huang X M, Ma L N, Zong W Y, Li M, Tang C. Determination of three-dimensional collision restitution coefficient of oil sunflower grain by high-speed photography. *Transactions of the CSAE*, 2020, 36(4): 44–53. (in Chinese)
- [3] Chen Z Q, Li Z F, Xia H H, Tong X. Performance optimization of the elliptically vibrating screen with a hybrid MACO-GBDT algorithm. *Particuology*, 2021, 56: 193–206.
- [4] Yin Z J, Zhang H, Han T. Simulation of particle flow on an elliptical vibrating screen using the discrete element method. *Powder Technology*, 2016, 302: 443–454.
- [5] Liu C S, Wang H, Zhao Y M, Zhao L L, Dong H L. DEM simulation of particle flow on a single deck banana screen. *International Journal of Mining Science and Technology*, 2013, 23(2): 273–7.
- [6] Yang X, Zhao L, Li H, Liu C, Hu E, Li Y, Hou Q. DEM study of particles flow on an industrial-scale roller screen. *Advanced Powder Technology*, 2020, 31: 4445–4456.
- [7] Wang L J, Cui Y Q, Zheng Z H, Feng X, Shen B S, Li Y B. Effect of different motion forms of vibrating screen on screening of particle group. *Transactions of the CSAM*, 2019, 50(6): 119–129. (in Chinese)
- [8] Xiao J Z, Tong X. Characteristics and efficiency of a new vibrating screen with a swing trace. *Particuology*, 2013, 11(5): 601–606.
- [9] Harzanagh A A, Orhan E C, Ergun S L. Discrete element modelling of vibrating screens. *Minerals Engineering*, 2018, 121: 107–121.
- [10] Ma Z, Li Y M, Xu L Z. Discrete-element method simulation of agricultural particles' motion in variable-amplitude screen box. *Computers and Electronics in Agriculture*, 2015, 118: 92–99.
- [11] Zhao L L, Zhao Y M, Bao C Y, Hou Q F, Yu A B. Optimisation of a circularly vibrating screen based on DEM simulation and Taguchi orthogonal experimental design. *Powder Technology*, 2017, 310: 307–317.
- [12] Feng X, Gong Z P, Wang L J, Yu Y T, Liu T H, Song L L. Behavior of maize particle penetrating a sieve hole based on the particle centroid in an air-screen cleaning unit. *Powder Technology*, 2021, 385: 501–516.
- [13] Wang Y, Yu J Q, Yu Y J, Zhang Q. Validation of a coupled model of discrete element method with multibody kinematics to simulate the screening process of a swing-bar sieve. *Powder Technology*, 2019, 346: 193–202.
- [14] Xia H H, Xin T, Li Z F, Wu X Q. DEM-FEM coupling simulations of the interactions between particles and screen surface of vibrating screen. *International Journal of Mining and Mineral Engineering*, 2017, 8(3): 250–263.
- [15] Wang L J, Wu Z C, Feng X, Feng X, Li R, Yu Y T. Design and experiment of curved screen for maize grain harvester. *Transactions of the CSAM*, 2019, 50(2): 119–129. (in Chinese)
- [16] Liu C L, Wang Y L, Song J N, Li Y N, Ma T. Experiment and discrete element model of rice seed based on 3D laser scanning. *Transactions of the CSAE*, 2016, 32(15): 294–300. (in Chinese)
- [17] Wu M C, Cong J L, Yan Q, Zhu T, Peng X Y, Wang Y S. Calibration and experiments for discrete element simulation parameters of peanut seed particles. *Transactions of the CSAE*, 2020, 36(23): 30–38. (in Chinese)
- [18] Ghodki B M, Patel M, Namdeo R, Carpenter G. Calibration of discrete element model parameters: soybeans. *Computational Particle Mechanics*, 2019, 6: 3–10.
- [19] Yuan J B, Wang J F, Li H, Qi X D, Wang Y J, Li C. Optimization of the cylindrical sieves for separating threshed rice mixture using EDEM. *Int J Agric & Biol Eng*, 2022, 15(2): 236–247.
- [20] Zhou L, Yu J, Liang L, Yu Y, Yan D, Sun K, Wang Y. Study on key issues in the modelling of maize seeds based on the multi-sphere method. *Powder Technology*, 2021, 394: 791–812.
- [21] Shen G L, Chen Z Q, Wu X Q, Li Z F, Tong X. Stepwise shape optimization of the surface of a vibrating screen. *Particuology*, 2021, 58: 26–34.
- [22] Gao X J, Cui T, Zhou Z Y, Yu Y B, Xu Y, Zhang D X, Song W. DEM study of particle motion in novel high-speed seed metering device. *Adv. Powder Technol*, 2021, 32(5): 1438–1449.
- [23] Qiao J P, Duan C L, Jiang H S, Zhao Y M, Chen J W, Huang L, et al. Research on screening mechanism and parameters optimization of equal thickness screen with variable amplitude based on DEM simulation. *Powder Technology*, 2018, 331: 296–309.
- [24] Di Renzo A, Di Maio F P. Comparison of contact-force models for the simulation of collisions in DEM-based granular flow codes. *Chem. Eng. Sci.*, 2004, 59(3): 525–541.
- [25] Dun G Q, Mao N, Gao Z Y, Wu X P, Liu W H, Zhou C. Model construction of soybean average diameter and hole parameters of seed-metering wheel based on DEM. *Int J Agric & Biol Eng*, 2022, 15(1): 101–110.
- [26] Li X Y, Du Y F, Mao E R, Zhang Y A, Liu L, Guo D F. Design and experiment of corn low damage threshing device based on DEM. *Int J Agric & Biol Eng*, 2023, 16(3): 55–63.
- [27] Long S F, Xu S M, Zhang Y J, Zhang J, Wang J. Effect of modeling parameters on the mechanical response of macroscopic crushing of agglomerate. *Powder Technology*, 2022, 408: 117720.
- [28] Hao J J, Wei W B, Huang P C, Qin J H, Zhao J G. Calibration and experimental verification of discrete element parameters of oil sunflower seeds. *Transactions of the CSAE*, 2021, 37(12): 36–44. (in Chinese)
- [29] Long, S F, Wei W B, Li D F, Kang S, Wang J. Study on separation of the tuber-soil binary mixture based on vibration and airflow coupling. *Biosystems Engineering*, 2024, 239: 13–24.
- [30] Zhou H L, Hu Z Q, Chen J G, Lv X, Xie N. Calibration of DEM models for irregular particles based on experimental Check for design method and bulk experiments. *Powder Technology*, 2018, 332: 210–223.
- [31] Roessler T, Katterfeld A. Scaling of the angle of repose test and its influence on the calibration of DEM parameters using upscaled particles. *Powder Technology*, 2018, 330: 58–66.